Serbian Tribology Society

SERBIATRIB '19

16th International Conference on Tribology

Faculty of Engineering University of Kragujevac

Kragujevac, Serbia, 15 – 17 May 2019

METHODOLOGY DEVELOPMENT OF AN IMPACT ABRASION TEST WITH VALIDATION BY COMPARISON WITH REAL INDUSTRIAL CASE

Haithem BEN HAMOUDA[1], Michiel CORRYN[1,*]

[1]ArcelorMittal Global R&D Gent - OCAS NV, Zwijnaarde, Belgium

*Corresponding author: michiel.corryn@arcelormittal.com

Abstract: *A testing methodology is proposed to simulate wear in dry conditions with a high-stress impact level. The studied impact abrasion test is known as the impeller-tumbler test. A methodology for this test was established based on a parametric study in order to investigate the corresponding influence on wear results. The rotation speed and the filling ratio of the abrasive particles were identified to have the highest influence on wear results, controlling the impact energy level on the material surface. Further parameters such as the particle size/type and contact duration were also inspected. Once stabilized, the methodology was applied on two industrial cases: stone crusher hammers from mineral processing and chute tour plates in mining application. Results for the first application showed wear mechanisms occurring on different positions of the HSI crusher hammers that are similar to the mechanisms observed on the impeller-tumbler abraded samples surface. For the mining application, a quantitative comparison of the wear rates was done showing a second validation case for the impact test. Finally, a predominant edge-concentrated wear was identified for all materials and was quantified using a 3D geometry reconstruction method.*

Keywords: *impact, abrasion, wear mechanism, 3D reconstruction, edge cutting, hammer mill, mining.*

1. INTRODUCTION

Abrasion is a major issue for component failure in applications such as mining, conveying and crushing of rocks. Selecting the most appropriate material for these applications is important to limit the high cost of repair and/or replacement and extending the component service life. For this purpose, accelerated abrasion tests are generally used to compare material performance. A reliable test methodology should give not only repeatable and reproducible results but also a representative ranking in the real application. In this work, the methodology developed to study materials abrasion performance under impact condition is detailed. A parametric study was done to investigate the test sensitivity. Finally, a comparison of this test to two test cases was done.

2. EXPERIMENTAL PROCEDURE

2.1 The impeller-tumbler test set-up

The impeller-tumbler was designed to simulate wear in dry conditions with a high-stress level and an impact abrasion mode. The test concept is not new and has been used in several references [1,2].

Figure 1 illustrates the working concept of the impeller tumbler test in dry condition. The test consists of two main components rotating independently: the tumbler and the impeller.

The impeller has a rotation speed of around 800 rpm while the tumbler is rotating at significantly lower rotation speed (about 50 rpm). The abrasive particles are placed in the tumbler and are continuously agitated by its rotation. The impeller is playing the role of sample holder holding simultaneously three samples and it rotates them to ensure impact contact with abrasive particles. The linear velocity of the samples can reach 38m/s.

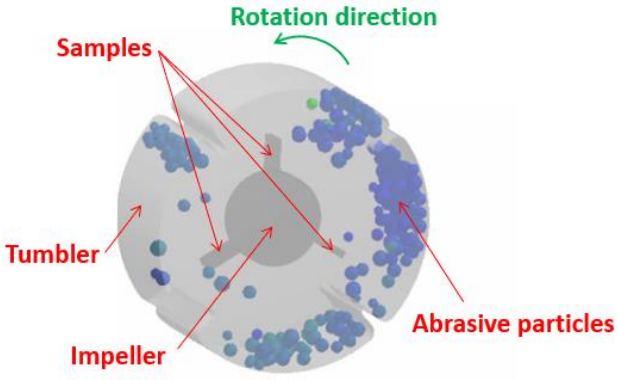

Figure 1. Schematic presentation of the impeller-tumbler

Table 1. Overview of influencing parameters

Parameter	Check
Abrasive particles	Size distribution of particles
	Fine versus coarse particles
	Renewal frequency
	Crushability of particles
Test duration	Transient and steady state regime
Samples	Position in holder
	Preparation
Rotational speed	Impeller speed
	Tumbler speed

Several test parameters were selected for test sensitivity analyses (Table 1). Preliminary parameter values were selected near the machine maximum capabilities in terms of speed and filling ratio. For the test duration, 3 hours was selected.

2.2 Material description

The reference material that was proposed in this study is a typical quenched fully martensitic steel with a Brinell hardness of 470, also referenced to as material A. In addition to this hard material, a soft pearlitic material was also studied (material B). An overview of the key mechanical properties of both materials is given in Table 2.

Table 2. Key properties of the reference materials

Material	Hardness [HBW]	Elongation [%]
Martensitic (A)	470	8
Pearlitic (B)	190	25

The samples were ground on all sides to prevent influences of sample geometry or roughness. The wear performance of both materials is analysed in the following sections.

2.3 Wear analyses methods

Wear losses were measured by mass loss obtained on a Mettler Toledo XSR603S precision balance with a repeatability of 0.5 mg. Mass losses were converted to volume losses by means of the density. Density values were obtained on the same balance using a corresponding density measuring kit.

A Field Emission Gun - Scanning Electron Microscope (FEG-SEM) was used for high-magnification observations of the worn surfaces. The model used in this work is a JEOL JSM-7001F SHL, with a magnification range of 10x to 10^6x.

A Taylor Hobson Talysurf CCI-HD, a non-contact surface roughness tool, was used to measure surface roughness parameters in accordance to ISO 22178-2. Topographical representation of a surface can be obtained with a vertical resolution of 0.1 nm over a full scan range plus a 0.4 µm lateral resolution.

To produce micro-hardness profiles, a Future Tech FM300 was used. Micro-Vickers values (HV 0.025) were accurate within 1% according to the latest calibration following ISO 6507-2.

A LK Evolution Coordinate Measuring Machine (CMM) was used to reconstruct the worn samples in 3D in accordance to ISO 10360-2. The CMM has a resolution up to 0.0023 mm.

3. RESULTS AND DISCUSSION

3.1 Effect of tribological parameters

The first test was performed on three reference material samples using the preliminary test parameters. Coarse, as-received granite particles (8-16mm) were used as abrasive. In this test, the goal is to observe the influence of the particle size distribution of the abrasive on the repeatability of the measurement. This could be observed by measuring the weight loss on the reference samples at every renewal of the abrasive. From the measurements on the three samples of the same material, the average volume loss was calculated at each time step (Fig. 2).

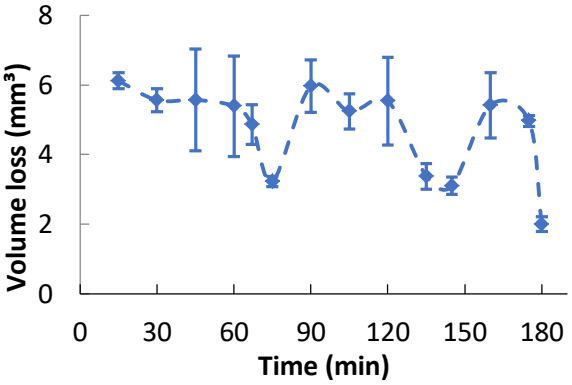

Figure 2. Volume losses at each time step for material A tested with abrasive as received

Figure 2 shows clear differences on the volume losses with high standard deviation especially in the time range of 40-120min. This shows a clear batch effect on the test results, which can be attributed to differences in the particle size distribution.

A close investigation of the abrasive particles shows the existence of several particles with significantly high aspect ratios. In fact, although the abrasive is sieved using standard sieves in the range of 8-16mm, some particles with a higher dimension can pass through the 8-16mm mesh due to their aspect ratio, leading to less homogeneous batches. Therefore, for every following test the abrasive batches were controlled by removing particles with high aspect ratio.

The second test repeated the conditions of the first test. However, now with the control of the abrasive particles' aspect ratio implemented. This test was repeated three times to obtain 9 measurements on the material A. The wear loss evolution showed a better fit to a linear tendency. The wear rate reduced slightly due to the removal of the heavier, high aspect ratio particles. However, for some points higher errors are observed in the beginning of the test (Fig. 3).

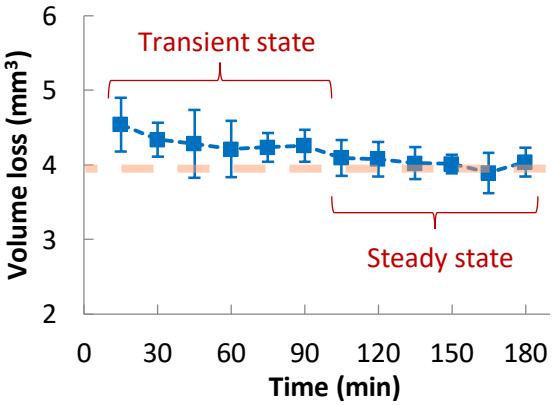

Figure 3. Volume losses at each time step for material A tested with controlled abrasive

A transient/running-in state was observed which was not clear from the preliminary test. During this initial state, a higher volume loss is combined with a higher error. Both reduce until around 100 minutes, where a steady state is reached. The final obtained error (averaged over the 9 tested samples) after 3 hours testing was around 3%. Such error value is lower than the acceptability criterion fixed in the ASTM-G65 standard test which is equivalent to 7% [3]. The initial higher wear can be attributed to the edge cutting effect, further elaborated in the next Section.

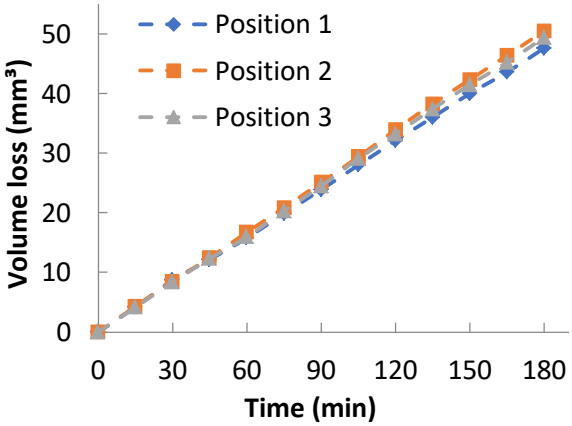

Figure 4. Cumulative volume losses for material A tested without sample rotation

Looking at the individual results from the same test, there is a difference in the volume

loss between the three reference samples at different positions (Fig. 4). The difference between the curves increases with time, reaching a value of almost 4% after 3 hours. A possible explanation is the possible size deviations between the machine slots that hold the samples.

To assess this, the test was repeated, but with the additional step of changing the sample position every time the abrasive was renewed in a way to get the same testing time in each slot. This procedure is called sample rotation and the results are presented in Fig. 5. With this procedure, the difference between the samples was less than 1% averaged over 3 tests. Consequently, one can conclude that slot differences exist and can be supressed by rotating the samples. This enables better comparison of the different materials in the same test by deleting effects linked to slot geometry.

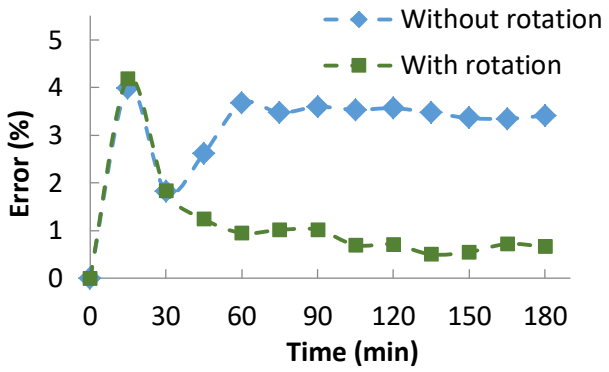

Figure 5. Volume losses at each time step for material A

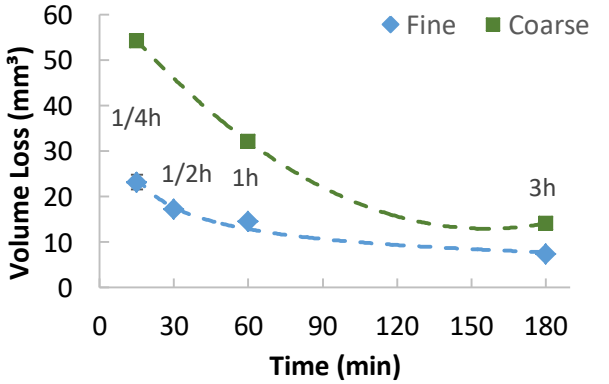

Figure 6. Cumulative volume losses for material A in function of abrasive renewal time step

The renewal of the abrasive batch every 15 minutes is an operator intensive task. Therefore, a study on the abrasive changing frequency was performed. The time step was varied from 15 minutes to 3 hours. The resulting cumulated volume loss after 3 hours, for both the fine and coarse granite, is plotted in function of the time step in Fig. 6.

The results show that increasing the time step to renew the abrasive batch, decreases the volume losses. This can be explained by the rounding of abrasive particles due to impact with the sample surface. This leads to a lower capability to remove material. This particle property is known as abrasiveness, which is linked to rock hardness, shape and sharpness [4]. For the coarse granite, this effect is more noticeable, with the volume loss for the ¼ hour time step being 69% higher than for a one hour time step and 284% higher than for a three hour time step.

The decrease in volume loss is non-linear. There is a steep decrease between the different time steps smaller than 1 hour. This can be explained by a fast degradation of the abrasive particles by breakage of the sharp edges. Once rounded, the particles have reduced size and limited abrasivity which can explain the obtained lower volume losses.

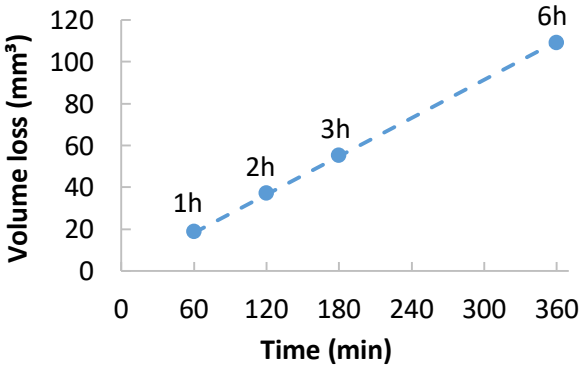

Figure 7. Cumulative volume loss for material A in function of experiment total duration

The aforementioned observations about the transient state, sample rotation, and abrasive renewal time step need to be considered before fixing the test duration. First, the test duration needs to be selected in the steady state regime to reach optimal accuracy. For reference material A, the steady state regime was established after almost two hours. Therefore, three hours might be an acceptable choice. Secondly, the time step of sample rotation (and abrasive renewal consequently) needs to be captured 3 or a

multiple of 3 times to have even time in each sample slot. A test was performed with a duration of 6 hours, see Fig. 7. This shows that the linear tendency is respected in longer tests. Therefore, an optimized wear test does not need longer durations and can be extrapolated using the linear tendency.

The rotation speed of the impeller controls the impact energy at which the particles encounter the material surface. This is also the influenced by the particle weight. As such, fine granite particles (4-8 mm) have a lower impact energy than coarse granite particles. Both granite abrasives were tested under two different rotation speeds of the impeller. The results are plotted in Fig. 8. Indeed, by increasing the impeller speed from 50% to 90% of the maximum rpm resulted in an increase of the cumulated volume loss by a factor of 3 to 4. The size effect is demonstrated in the same figure as well. Both have a significant effect and can be used as a tuning parameter to control the impact energy induced on the material surface.

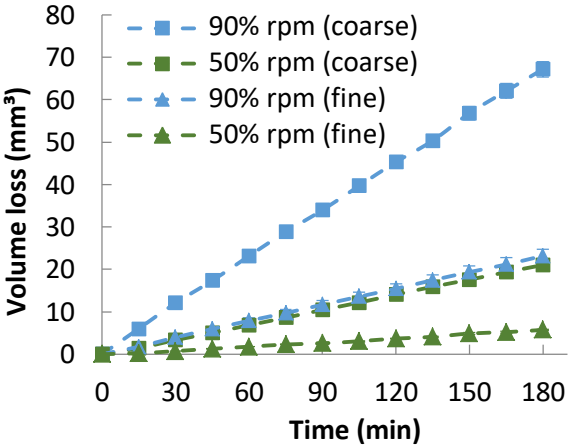

Figure 8. Cumulative volume losses for Material A in function of abrasive size and impeller rpm

The rotation speed of the tumbler can be controlled in a range to about 50 rpm. This rotation is necessary to agitate the particles. The effect of increasing the tumbler speed from a low value, to 3 times this value is represented in Figure 9. By increasing the rotation speed of the tumbler, the volume moss measured after 3 hours has increased by 87%. This increase in speed resulted in a higher agitation of the particles, leading to more impacts. However, a further increase will lead to less impacts due to centrifugal forces.

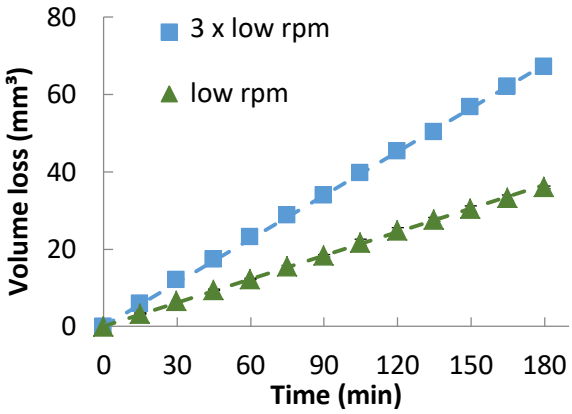

Figure 9. Cumulative volume losses for Material A in function of tumbler rpm

Another factor related to the abrasive particles is the crushability. Due to the high stress conditions, wear occurs in both the abrasive and the tested sample. For the abrasive, the wear test could play the role of a rock crusher, especially if the sample material has a high hardness. The abrasive renewal time step was reduced to prevent too much rounding of the particles. However, the sample hardness has an influence on the crushability of the particles and may make it not representative to compare results for materials with another hardness.

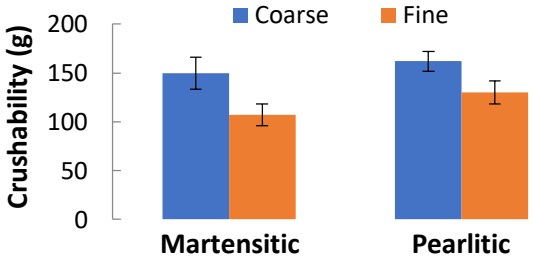

Figure 10. Crushability measured as mass loss of the abrasive particles during a time step tested on Material A and B

Measuring the weight loss of the abrasive particles after each time step gives an indication about the abrasive particles' crushability. For this study, two types of abrasives are studied: coarse and fine granite particles. The different stones were extracted from different quarries, so a risk of different hardness and crushability is possible. These were tested with two types of "crusher blades": reference material A (martensitic, 470 HBW) and material B (pearlitic, 190 HBW). Figure 10 shows the result of this comparison. For the

same abrasive, there is no observed influence of the sample hardness on the particle crushability. However, the fine particles show a lower crushability than the coarse particles. This corresponds to the observations in Figure 6, where the renewal step time had less influence on the fine particles.

Table 3. Influencing parameters of the impeller-tumbler test

Parameter	Influence
Rotation speed impeller	From 50 to 90% of max rpm → Volume Loss times 3
Rotation speed tumbler	<10 rpm → Bad abrasive mixing (no impacts) >50 rpm → Less impacts
Abrasive changing time step	> 1h → Lower abrasiveness < ¼ h → Higher cost
Test duration	<2h → Steady state not reached >3h → gives no further information
Abrasive size	From fine to coarse particles → Volume Loss times 3
Abrasive particles distribution	Influences linear tendency
Sample position	Different results per position

The sensitivity of each influencing parameter was examined. Table 3 gives a summary of these with their influence on the test result.

3.2 Wear mechanisms

Samples subjected to the impeller tumbler were studied using various techniques with the aim to characterise the wear mechanisms at play. This was done for the hard reference material A and the softer material B to observe a probable change in mechanism.

From a visual inspection, one can remark that the contact surface is severely impacted at the edges, resulting in a rough surface. The edges are rounded as well. For the softer material, material was visibly ploughed to the edges, forming a burr. Also visible, is a decrease in impact density going from the edge to the impeller slot. Therefore, different locations were marked to see the difference in behaviour, see Fig. 11.

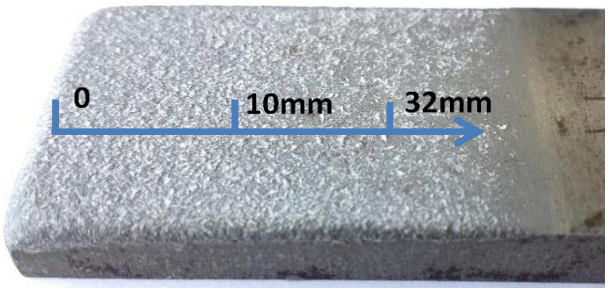

Figure 11. Sample with rounded edges and locations marked on sample

The FEG-SEM micrographs showed a severely deformed edge at position 0, characterized by a rough surface with a high density of craters/peaks on both materials. Close to the impeller slot, at 32 mm distance, localized deformation areas are visible. This could be attributed to single impacts of the abrasive particles.

At a higher magnification, embedded abrasive particles were visible on both materials. For the martensitic grade, small wear particles have been identified on the worn surface of the martensitic grade in Fig. 12. These particles, known as chips or chunks, are formed due to the cutting of material that was previously folded by plastic deformation to form the wedge of the crater/groove. This wear feature is characteristic of the micro-cutting mechanism.

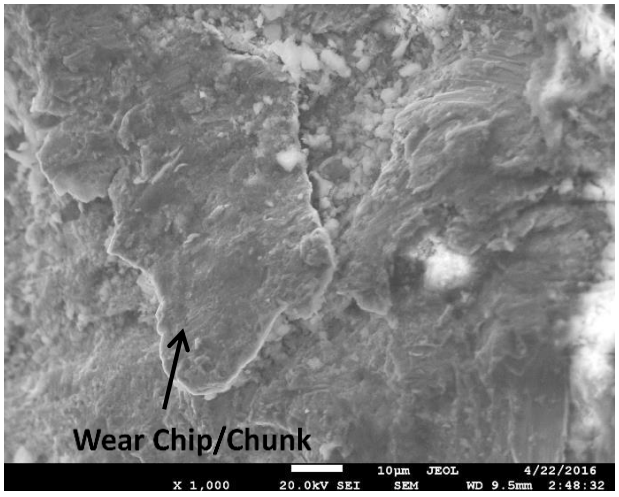

Figure 12. FEG-SEM of chunk particle in material A

Micrographs on the cross-section areas showed wavy patters with fibered substructures.

The observed waviness is more developed for the soft pearlitic material and could be defined as a superposition/folding of heavily deformed material chunks after subsequent impacts of the abrasive particles (Fig. 13). This mechanism is known as microstructure micro-forging by impact of abrasive particles. This observation was confirmed by EDX analysis which identified the presence of dust of abrasive grains.

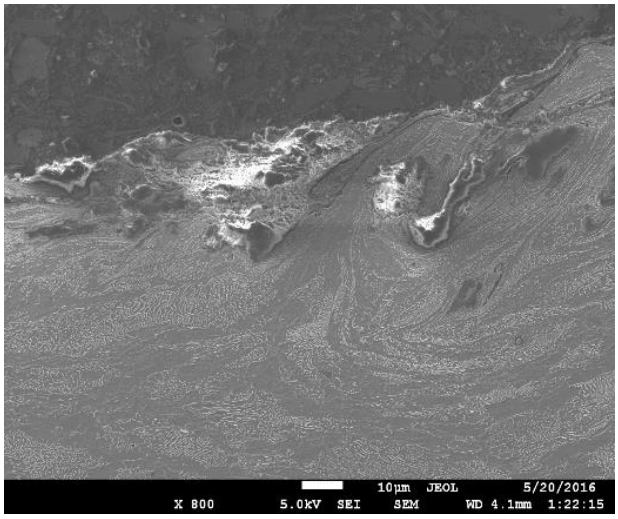

Figure 13. FEG-SEM of waviness in material B

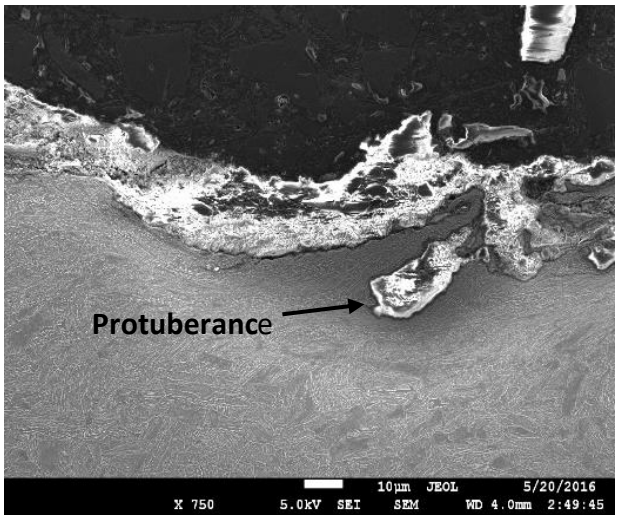

Figure 14. FEG-SEM of protuberance on material A surface

For the martensitic material, material folding/displacement was limited due to the lower strain hardening capability. This can explain the existence of maximum one layer/wave of folded material (protuberance) in the material surface because further deformation will lead to cutting of the protuberance to form a chunk/chip. This feature has been already identified for similar test conditions in previous research studies [1,2], see Fig. 14.

At a distance of 32mm far from the edge, no waviness is observed for any of the tested materials which can be explained by only single impacts present in this area. However, embedded particles are identified in the craters that were formed. This allows for a measurement of the penetration depth of a single particle: around 48 µm (Fig. 15).

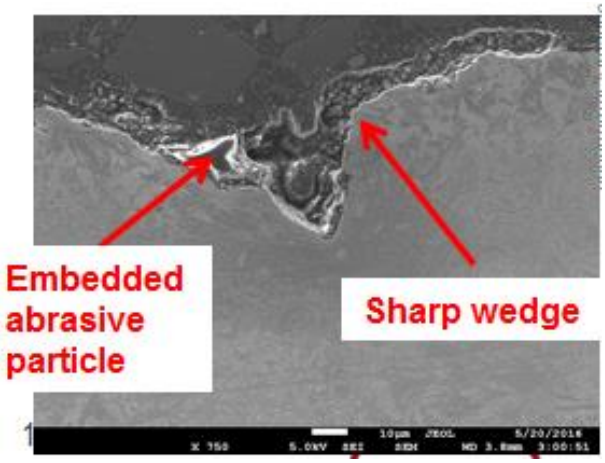

Figure 15. FEG-SEM of embedded particle in material A

To validate the micrographic analysis, surface profilometry was performed. The root mean square height parameter (S_q) is a stable indicator of the surface roughness. The evolution of this parameter for both samples is given in Fig. 16. For material B, there is a clear evolution from a rough surface at the end to a smoother surface near to the impeller slot. On the harder material A, the change is negligible.

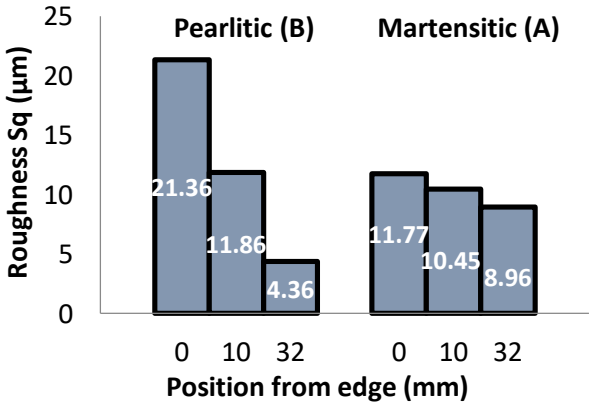

Figure 16. S_q at marked locations for both material A and B

Micro-hardness profiles were extracted as well. The aim was to observe the subsurface structures' hardness. During subsequent impacts by multiple abrasive particles a plastic strain

gradient is formed progressively underneath. The maximum strain is found at the particle-sample interface; it decreases continuously with increasing depth and ultimately reaches zero at the elastic-plastic boundary. The thickness of this gradient in known as the subsurface hardened layer/lip generally characterized by deformed/elongated grains beneath the wear track (groove and crater).

For the pearlitic material, the micro-hardness cross-section profile is plotted in Fig. 17. The profiles representing the edge and the middle position show a hardening gradient beneath the contact surface. At the 0 mm position, a maximum hardness of around 350 HV was reached with a gradient of about 500 µm. At the 10 mm position this was 280 HV with a gradient of about 200 µm. Near the sample holding slot no hardening was observed, the measured values oscillate around the bulk hardness.

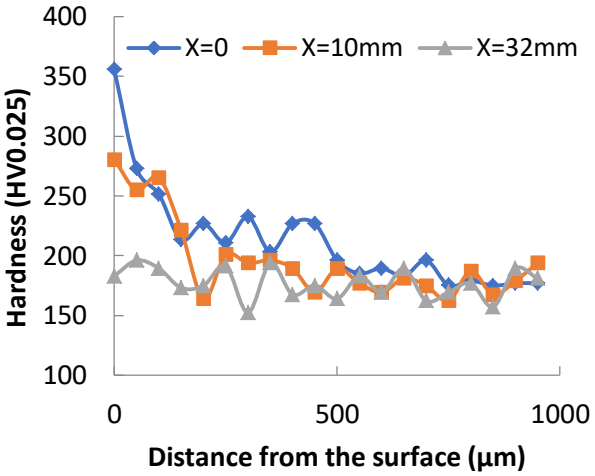

Figure 17. Cross-section micro-hardness profiles for the pearlitic grade

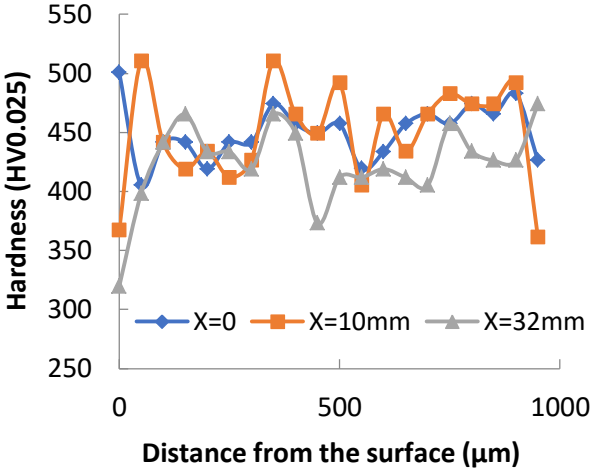

Figure 18. Cross-section micro-hardness profiles for the martensitic grade

The profiles measured on the martensitic grade do not show a clear hardness at any location (Fig. 18). As the step size of the measurement is 50 µm, it is possible that the layer was not measured. Observed from SEM images, the layer can be visually estimated to be around 5 µm thick.

The cross-thickness hardness profiles confirmed the wear mechanisms involved for both material A and B under high stress impact abrasion conditions. Micro-cutting is the main mechanism in the martensitic material, resulting in a thin hardened layer with a low fibering capacity. For the pearlitic material this is plastic deformation, therefore it develops a thick hardened layer/lip and shows a high fibering capacity.

Finally, a CMM was used to reconstruct the worn samples in 3D. The aim was to quantify how much the edge effect contributes to the total mass loss. Therefore, the reconstructed samples were divided into two parts defining the edge and inner part (Fig. 19). On the reference material A, about 85% of the total wear occurred at the sample edges. This was the case with both fine and coarse abrasive.

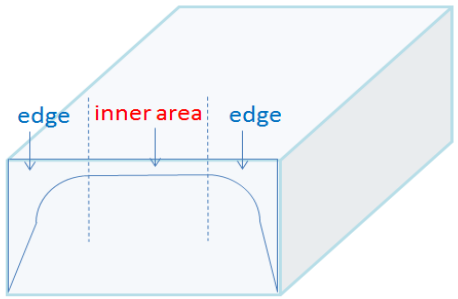

Figure 19. Separation of edge and inner area

With the wear mechanisms in mind for both materials, one could expect that the softer material would have a higher wear resistance due to the capability to absorb multiple impacts by plastic deformation. Therefore, both were subjected to an impeller-tumbler test using fine granite, see Fig. 20. The martensitic grade showed a linear behaviour due to the stable micro-cutting mechanism. However, the pearlitic material showed a wear behaviour in two stages. The first stage was very similar to the martensitic grade; the wear rate increased in the second stage. This change must be marked by a change in wear mechanism.

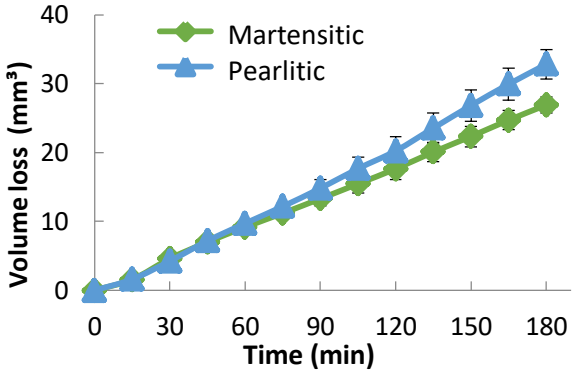

Figure 20. Cumulative volume losses for Material A and B

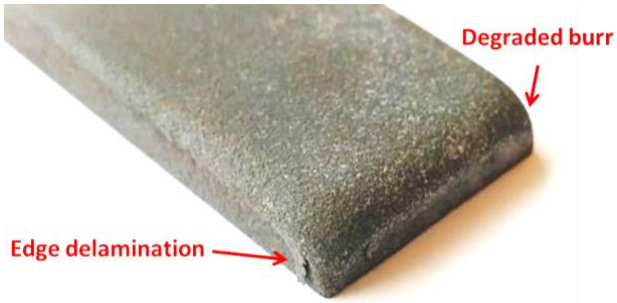

Figure 21. Edge delamination on the pearlitic material

After inspection of the soft material, the change in mechanism was observed. In the first phase, a burr is formed as a result of plastic deformation, as visible in Fig. 21. This burr keeps being developed as long as the material work hardening is not fully consumed at the edges. At a given time, the surface is fully hardened, and the formed burrs become large enough to be delaminated. This mechanism can explain the increase in wear rate in the second stage.

4. APPLICATION TO MINING CASES

The impeller-tumbler test is an edge concentrated wear test. Such edge effect is also existing in many other wear tests and applications exhibiting sharp contact surfaces. Therefore, it can be applied to various industrial cases with sharp contact surfaces. The test will be validated against two such cases.

4.1 HSI hammer crusher

An industrial case needed to be selected to validate the test procedure. A failed hammer from a limestone crusher was received. The part rotated at the edge of a spinning rotor wheel of almost 4 meters with the aim to crush limestone by impact. This part was mostly martensitic and will be subjected to a wear analysis.

By comparison of the occurring wear mechanism to the ones observed in our tests, a first validation of the developed method was made possible. When visually inspected, the received sample shows a worn edge and a rough surface. Again FEG-SEM, profilometry and hardness profiles will be used to further investigate the failure mechanism.

From the FEG-SEM images, it was shown that the worn middle section exhibited single craters. The craters were followed by grooves. This suggests that the impact occurred at low impingement angles. At the edge, the hammer showed a high number of craters. A cross-section showed the presence of protuberances piled up at the crater's wedge due to multiple impacts on the material surface at that position (Fig. 22). These features are similar to what was observed at the middle and edge of the martensitic sample worn by the impeller-tumbler test.

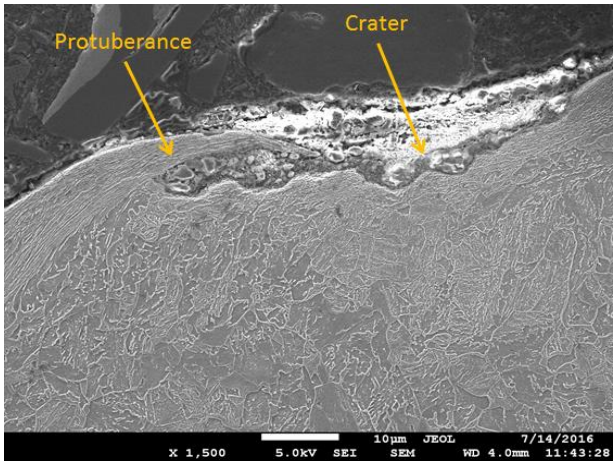

Figure 22. FEG-SEM of protuberance on hammer surface

The two other used techniques again showed results very similar to the observations on the test samples. The Hardness profiles did not show any hardening. However, the SEM images showed a gradient layer that was a few micrometres thick. Profilometry proved a higher roughness at the edge compared to the middle section.

4.2 Chute tour plates

A mining chute part was received in two materials, a martensitic material with a hardness of 400 HV and a similar material of 500 HV. Both had the same usage history. As such, their wear resistance could be compared. Impeller-tumbler samples were made from the same materials.

To compare the wear obtained in the application and the test, the life time was used. This unitless number compares the material wear resistance to a chosen reference material's resistance. The wear rate must be calculated first with the measured volume loss (VL), the area subjected to wear (WA), and the duration of the wear process (t). The calculation is laid out in formulas (1) and (2).

$$Wear\ rate\ \left[\frac{\mathrm{mm}}{\mathrm{s}}\right] = \frac{VL\ [\mathrm{mm}^3]}{WA\ [\mathrm{mm}^2] \times t\ [s]} \quad (1)$$

$$Life\ time = \frac{Wear\ Rate_{400\ HV}}{Wear\ Rate_{500\ HV}} \quad (2)$$

Table 4 shows the resulting values for both the field components and the lab samples. The good matching of the data indicates a successful choice of the test procedure to simulate the material life time in-service.

Table 4. Life time results

Test	Life time
Field	0.77 to 0.93
Lab	0.87

5. CONCLUSION

A wear testing methodology was detailed in this work showing different influence on the test results. Particle size and impeller rotation speeds were considered to be the most influencing parameters affecting directly the impact energy applied on the material. Moreover, characterization techniques showed the edge concentration wear in this test and the predominant impact abrasion mechanism.

The wear mechanism observed on the samples worn by the tumbler-impeller correspond to the mechanisms observed in the two selected mining applications. It was possible to obtain a material performance ranking representative of the application as well. As such, the test can be used to assess material performance and failure modes in application.

REFERENCES

[1] R. Wilson, J. *Hawk: Impeller wear impact-abrasive wear test*, Wear, Vol. 255-229, pp. 1248-1257, 1999.

[2] V. Ratia et al.: *High-Stress Abrasion and Impact-Abrasion Testing of Wear Resistant Steels*. s.l., s.n., 2011.

[3] ASTM G65-15 *Standard Test Method for Measuring Abrasion Using the Dry Sand/Rubber Wheel Apparatus,* 2015.

[4] G. Pintaude, M. Coseglio: *Severe metallic wear*, in: *Proceedings of 20th International Congress of Mechanical Engineering*, 15-20.11.2009, Gramado, Brazil.